Synthesis of poly(ethyleneimine)s–silica hybrid particles with complex shapes and hierarchical structures†

Ren-Hua Jin* and Jian-Jun Yuan

Received (in Cambridge, UK) 16th November 2004, Accepted 10th January 2005
First published as an Advance Article on the web 26th January 2005
DOI: 10.1039/b417351a

Shaped silica constructed by silica fiber with axial poly(ethyleneimine)s (PEIs) filaments was available simply from rapid hydrolytic condensation of tetramethoxysilane (TMOS) upon aggregates of PEIs with different architecture.

Silica skeletons in biosilicas such as sponges and diatoms grow rapidly with the formation of beautiful shapes and precise patterns at ambient conditions. To reproduce artificially the mimicking of these architectures is one of the main targets of material scientists.[1] It has been demonstrated that in biosilicification of diatoms, polyamine is one of a set of key molecules, which may participate in the formation of biosilica patterns.[2] In the field of the biomimetic synthesis of silica, polyamines[2–5] including synthesized polymers and native/modified biopolymers such as poly(L-lysine), poly(L-lysine-b-L-cystein), amine-terminated dendrimers, branched poly(ethyleneimine), poly(allylamine)-hydrochloride, N-methylated poly(propyleneimine), silaffin peptides have been used for the shape control of silica. However, these polyamines often prefer to mediate spherical silica although individual non-spherical silica[3a,b] structures were developed. We describe in the present report how polyamines with different molecular shapes can direct the formation of silica-based hybrid structures with complex morphologies. Moreover, since little was known until now about the actual structure of polyamines in the resulting silica, we determined the structure of polyamines, once trapped into the silica framework.

PEIs with linear backbones are significantly different to their branched counterparts. Linear PEI is crystalline with a double helix or planar zig-zag conformations[6] depending on dehydrate or hydrate states, and is insoluble in water at room temperature. Here, three PEIs **1–3** (Scheme 1) with different architectures were used for silica deposition. The PEIs can immobilize water to form ice cream-like thermoreversible hydrogels (Fig. 1), which are sustained by the differently shaped crystalline aggregates depending on the PEI architecture. The four-armed star with a porphyrin core assembled into aster-like aggregates while the six-armed star with a benzene ring core produced fan-like fibrous bundles. The linear PEI resulted in branched fibrous bundles. We prepared a series of aqueous aggregates of the PEIs with different content ranging from 0.25 to 3% (wt%) for silica deposition. Surprisingly, the mixture of an ethanol solution of TMOS (rather than silicic acid) with the aqueous aggregates rapidly resulted in silica particles within 10 min without any additive catalysts at room temperature.

We visualized all the resulting silica particles by SEM (Fig. 2 and Figs. S2–S4, see ESI†). Interestingly, the silicas mediated from the aggregates of **1**, **2** and **3** showed aster (**1**Si), fiber-sponge (**2**Si) and leaf (**3**Si) morphologies, respectively. The **1**Si-a formed from the higher content of **1**(2%) have more than 5 arms which expanded towards three-dimensional directions (Fig. 2a, Fig. S2 see ESI†). Each arm on the aster silica becomes wider towards the outer and the end of the arm appears serrate. The silica **1**Si-b obtained from the lower content of **1** (0.25%) still retained the aster shape but the number of arms increased dramatically with formation of highly split twigs (Fig. 2b). Each twig is about 30 nm in width. For silica obtained with 2% of **2**, a fibrous framework **2**Si-c is clearly observed by SEM (Fig. 2c). A close observation (see insets) tends to prove that these fibers are themselves obtained by the aggregation of thinner nanofibers. When the concentration in **2** is decreased to 0.25%, changes in morphologies **2**Si-d (even if the fibrous structure is still preserved)

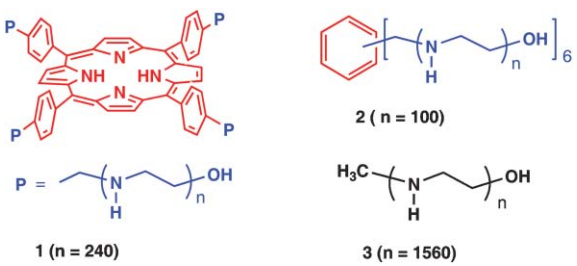

Scheme 1

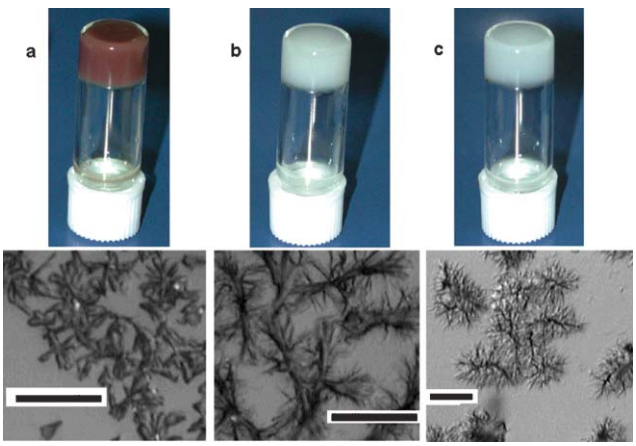

Fig. 1 Top: Photographs of hydrogel-like aggregates containing 1% of **1** (a), **2** (b) and **3** (c). Bottom: Optical microscope images observed from the hydrogel-like aggregates of a, b and c (from left), scale bar 10 μm. These differently shaped crystalline aggregates sustained the hydrogels.

† Electronic supplementary information (ESI) available: Experimental section and Figs. S1–S6. See http://www.rsc.org/suppdata/cc/b4/b417351a/

*jin@kicr.or.jp

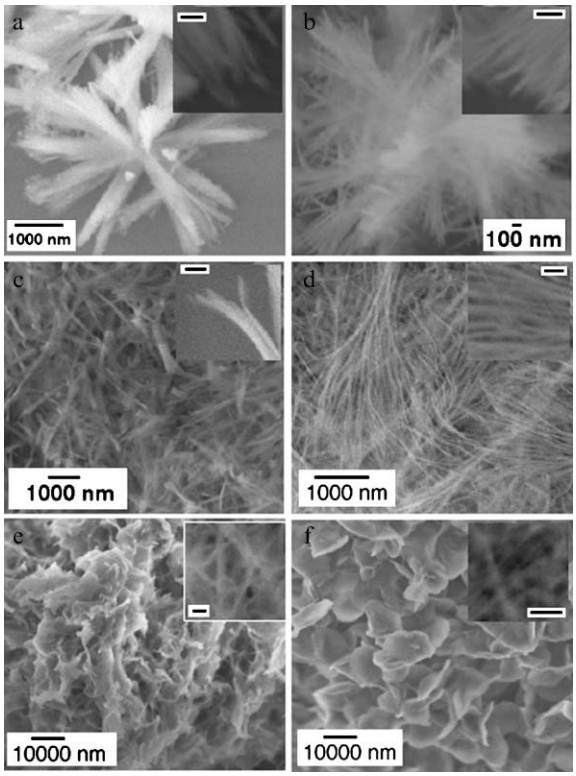

Fig. 2 SEM images of the shaped silicas. The silicas (a, c, e) and (b, d, f) were mediated at 2.0 and 0.25% concentrations of the polymers, respectively. (a, b) for the aster silicas, (c, d) for the sponge silica, (e, f) for the leaf silica. Insert: magnification images of the images of a–f, respectively. Scale in insert: 100 nm.

are observed. The silica particles (**3**Si-e and **3**Si-f) produced from the aggregate of **3** are different from the cases of the two star polymers (Fig. 2e–f and Fig. S4, see ESI†). The **3**Si-e mediated from 2% of **3**, are thin and expanded (Fig. 2e) whereas the silica **3**Si-f became thick and compact when mediated from 0.25% of **3** (Fig. 2f). In the thin **3**Si-e, it is clearly seen that many fibrils crossed each other (inset in Fig. 2e). In the thick **3**Si-f (inset in Fig. 2f), we observed that the fibrils crowded each other with formation of many pores (*ca.* 20–30 nm). This seems to be a nanofiber web. The fibers are also about 30 nm in width. In the formation of the above structured silicas, the silica deposition only occurred on the surface of the aggregates rather than in a continuous water phase. However, an aqueous molecular solution of branched PEI (even at very low concentration) resulted quickly in bulky silica without shape formation when it was mixed with TMOS. Thus we consider that the aggregates of the polymers are rod-like micelles with brush-like shell on the crystalline fiber surface. Probably, the PEI brush just strongly promotes the rapid hydrolytic condensation of TMOS. This expectation was supported from the other system where spherical polymeric micelles[7] consisted of a hydrophobic core and PEI corona rapidly induced the hydrolytic condensation of TMOS to give structured silica (data not shown). It appears from these observations that two factors affect the final morphology of the silica-polyamine hybrid materials. The main one remains the initial shape of the polyamine that directs the overall growth of the particles. The second parameter is the concentration (Fig. S2, see ESI†) of the template molecule that modifies in a second step, the fine structure of these materials. Its influence might arise from variations of the nucleation, growth kinetics and brush density in the aggregations. The formation of the aster structure silica from the star **1** would contribute to the effect of the stacking association of the porphyrin residues on the aggregation of the star (Fig. S5, see ESI†).

Furthermore, we tried to characterize the structure of the polymers once they are trapped in the silica fiber. The content of the polymers in the silica particles is about 25% in mass. From the solid state ^{13}C-NMR for the silica, we observed a single peak at 29.9 ppm, which was assigned to the methylene carbon (CH_2–N–CH_2) in the PEI chain. We further defined the state of the polymers in the silica by means of X-ray diffraction (XRD) and DSC. XRD patterns were recorded for the 3% aqueous aggregates of **1** to **3**. All exhibit three diffraction peaks at nearly the same angles (20, 27 and 28° in 2θ, also see ESI†) (Fig. 3a). These XRD patterns are similar to the reported PEI crystals with zig-zag conformation[6] which often form in the dihydrated state of the linear PEI (NCH_2CH_2/H_2O = 1/2). Surprisingly, XRD patterns of the hybrid compounds exhibit the same diffraction peak as those observed with pure amine aqueous aggregates (Fig. 3b). In DSC traces, melting peaks appeared clearly (Fig. S6, see ESI†). These results indicate that the PEIs in the silicas retain their crystallinity to a considerable extent. As mentioned above, the silicas with different shapes showed elementary silica fibers whose width are less than 30 nm. To clarify the relationship between the silica fiber and the PEI crystalline, the leaf-like silica was used in TEM observations. From Fig. 3c, evidently, the silica was constructed from many silica fibers forming a nanofiber web (consistent with SEM images in Fig. 1e and f). In the HR-TEM image gained from an isolated elementary fiber, it is remarkable that the gray wall coated the dark core (Fig. 3d). The fiber is *ca.* 25 nm and the core is 5–7 nm in width. This revealed that the silica shell just coats the axial filament of the crystalline PEI to form the elementary silica

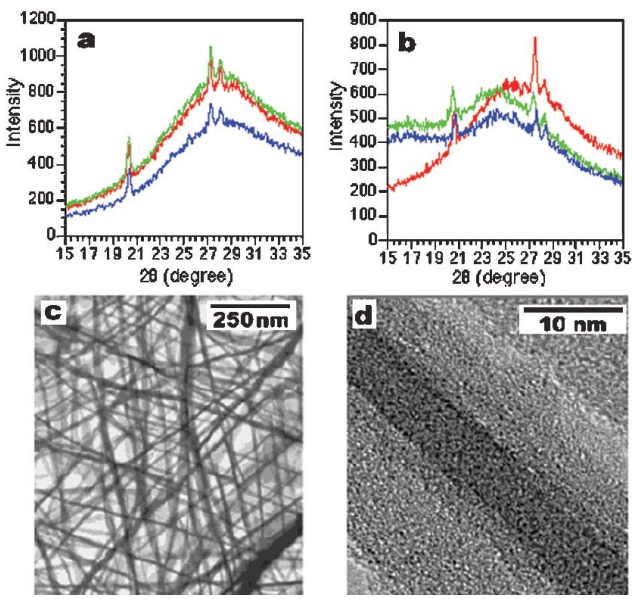

Fig. 3 XRD patterns of the polymers **1**–**3** in the aqueous aggregates (a) and in the silicas (b): blue for **1**; green for **2**; red for **3**. TEM images of the leaf-like silica (c) and high resolution TEM (HR-TEM) image of an isolated silica fiber with filament core (d).

fiber. Such silica formation is very similar to the demosponges of biosilica which grow *via* polymerization of silicic acid around an axial filament of proteins to give a silica fiber.[1,8]

We were able to control silicas into much more changeable shapes by tuning the PEI aggregates and were able to construct both nanometallic and nanotube structures within the shaped silicas (submitted for publication). We believe that our findings will provide straightforward insights for developing and constructing silicate materials.

Ren-Hua Jin* and Jian-Jun Yuan
Synthetic Chemistry Lab, Kawamura Institute of Chemical Research, 631 Sakado, Sakura, Chiba 285-0078, Japan. E-mail: jin@kicr.or.jp; Fax: (+81)43 498 2202

Notes and references

1 W. E. G. Muller, Ed. *Silicon Biomineralization: Biology-Biochemistry-Molecular Biology-Biotechnology*; Springer, Berlin, 2003.
2 N. Poulsen, M. Sumper and N. Kroger, *Proc. Natl. Acad. Sci. USA*, 2003, **100**, 12075–12080; N. Kroger, R. Deutzmann and M. Sumper, *Science*, 1999, **286**, 1129–1132; N. Kroger, R. Deutzmann, C. Bergsdorf and M. Sumper, *Proc. Natl. Acad. Sci. USA*, 2000, **97**, 14133–14138.
3 (*a*) J. N. Cha, G. D. Stucky, D. E. Morse and T. J. Deming, *Nature*, 2000, **403**, 289–292; (*b*) S. V. Patwardhan, N. Mukherjee, M. Steinitz-Kannan and S. J. Clarson, *Chem. Commun.*, 2003, 1122–1123.
4 (*a*) F. Rodriguez, D. D. Glawe, R. R. Naik, K. P. Hallinan and M. O. Stone, *Biomacromolecules*, 2004, **5**, 261–265; (*b*) S. V. Patwardhan and S. J. Clarson, *J. Inorg. Organomet. Polym.*, 2003, **13**, 49–53.
5 M. R. Knecht and D. W. Wright, *Langmuir*, 2004, **20**, 4728–4732; R. R. Naik, P. W. Whitlock, F. Rodriguez, L. L. Brott, D. D. Glawe, S. J. Clarson and M. O. Stone, *Chem. Commun.*, 2003, 238–239; T. Mizutani, H. Nagase, N. Fujiwara and H. Ogoshi, *Bull. Chem. Soc. Jpn.*, 1998, **71**, 2017–2022.
6 T. Hashida, K. Tashiro, S. Aoshima and Y. Inaki, *Macromolecules*, 2002, **35**, 4330–4336; Y. Chatani, H. Tadokoro, T. Saegusa and H. Ikeda, *Macromolecules*, 1981, **14**, 315–321.
7 R.-H. Jin, *Adv. Mater.*, 2002, **14**, 889–892; R.-H. Jin, *ChemPhysChem*, 2003, **4**, 1118–1121.
8 T. Coradin and P. J. Lopez, *ChemBioChem*, 2003, **4**, 251–259.